Divergence of riparian forest composition and functional traits from natural succession along a degraded river with multiple stressor legacies

Philippe Janssen, John C. Stella, Hervé Piégay, Bianca Räpple, Bernard Pont, Jean-Michel Faton, Johannes Hans C. Cornelissen, André Evette

Divergence of riparian forest composition and functional traits from natural succession along a degraded river with multiple stressor legacies

Janssen, Philippe[1,2]*, Stella, John C.[3], Piégay, Hervé[1], Räpple, Bianca[1], Pont, Bernard[4], Faton, Jean-Michel[4], Cornelissen, Johannes Hans C.[5], Evette, André[2]

[1] Univ. Lyon, UMR 5600 Environnement Ville société, CNRS, Site of ENS Lyon, Lyon, France

[2] Univ. Grenoble Alpes, INRAE, LESSEM, St-Martin-d'Hères, France

[3] Department of Forest and Natural Resources Management, State University of New York College of Environmental Science and Forestry, Syracuse, NY, 13210 USA

[4] Réserves Naturelles de France, Quétigny, France

[5] Department of Ecological Science, Faculty of Science, Vrije Universiteit Amsterdam, Amsterdam, The Netherlands

* Corresponding author, e-mail philippe.janssen@inrae.fr, phone +33 476762879

Email addresses of other authors:

J.C. Stella (stella@esf.edu), H. Piégay (herve.piegay@ens-lyon.fr), B. Rapple (b.raepple@yahoo.de), B. Pont (bernard.pont@cen-isere.org), J-M. Faton (jmfaton@lagaredesramieres.com), J.H.C. Cornelissen (j.h.c.cornelissen@vu.nl), A. Evette (andre.evette@inrae.fr)

Running head: Accelerated succession on degraded river

Abstract

Prolonged exposure to human induced-stressors can profoundly modify the natural trajectory of ecosystems. Predicting how ecosystems respond under stress requires understanding how physical and biological properties of degraded systems parallel or deviate over time from those of near-natural systems. Utilizing comprehensive forest inventory datasets, we used a paired chronosequence modelling approach to test the effects of long-term channelization and flow regulation of a large river on changes in abiotic conditions and related riparian forest attributes across a range of successional phases. By comparing ecological trajectories between the highly degraded Rhône and the relatively unmodified Drôme rivers, we demonstrated a rapid, strong and likely irreversible divergence in forest succession between the two rivers. The vast majority of metrics measuring life history traits, stand structure, and community composition varied with stand age but diverged significantly between rivers, concurrent with large differences in hydrologic and geomorphic trajectories. Channelization and flow regulation induced a more rapid terrestrialization of the river channel margins along the Rhône River and accelerated change in stand attributes, from pioneer-dominated stands to a mature successional phase dominated by non-native species. Relative to the Drôme, dispersion of trait values was higher in young forest stands along the Rhône, indicating a rapid assembly of functionally different species and an accelerated transition to post-pioneer communities. This study demonstrated that human modifications to the hydro-geomorphic regime have induced acute and sustained changes in environmental conditions, therefore altering the structure and composition of riparian forests. The speed, strength and persistence of the changes suggest that the Rhône River floodplain forests have strongly diverged from natural systems under persistent multiple stressors during the past two centuries. These results reinforce the importance of considering historical changes in environmental conditions to determine ecological trajectories in riparian ecosystems, as has been shown for old fields and other successional contexts.

Key-words: riparian forests, ecological succession, community-weighted traits, human induced-stressors, ecological trajectories

Introduction

The concept of ecological succession dates almost to the origins of the field of ecology itself. Over the last century, conceptual frameworks of how plant communities assemble (or re-assemble) following large perturbations have evolved from a focus on pattern to the underlying mechanisms, notably the feedbacks that occur between abiotic and biotic ecosystem components as they develop over time (Connell and Slatyer 1977, Pickett et al. 1987, Meiners et al. 2015). This shift in focus has come with an increasing appreciation of ecological complexity, particularly the effects of multiple interacting drivers and stressors, thresholds and other non-linear responses, and the importance of contingent factors (e.g., variation in historical management strategies or in the intensity and duration of management) in driving community trajectories (Clark et al. 2019, Chang and Turner 2019). Nevertheless, synthesizing general principles and testing predictions of ecological succession across diverse ecosystems remain a challenge. The recent focus on monitoring change in ecological traits, rather than species composition, in plant assemblages over time shows promise in distilling patterns and drivers of community dynamics in response to shifts in both extrinsic factors (e.g., disturbance, climate) and intrinsic ones (e.g., soil properties, competition) (Meiners et al. 2015, Chang and Turner 2019).

The trait-based approach is particularly well-suited for studying natural communities that are severely degraded by multiple, interacting human stressors; these include resource exploitation (e.g., overfishing), exotic species invasions, and changes in land use, climate and disturbance regimes due to human activities (Mouillot et al. 2013). As with natural disturbances, human-induced stressors can greatly alter ecological trajectories of both terrestrial and aquatic ecosystems, and lead to rapid and potentially irreversible shifts in ecosystems properties (Folke et al. 2004). Numerous studies document divergences in successional trajectories of species assemblages and functional traits between altered and reference ecosystems (e.g., Odion et al. 2010, Sfair et al. 2016, Clark et al. 2019), in many cases leading to alternative ecosystem states (Beisner et al. 2003). Strong shifts in species dominance during succession due to native biodiversity loss and/or invasion by exotic species may impede the ecological resilience of ecosystems, and compromise efforts to restore them or preserve their functions and services (Suding 2011).

Riparian ecosystems are among the most modified by human activities (Tonkin et al. 2018) and comprise some of the most vulnerable biomes to ongoing global change (Perry et al. 2012, Stella et al. 2013b). More than most forest ecosystems, riparian woodlands comprise a fragmented patch mosaic of diverse composition and age, which are related to strong physical gradients and flood history (Naiman and Decamps

1997, Scott et al. 1997, Bendix and Stella 2013). Abiotic conditions and plant species composition can change markedly within only a few decades during riparian succession (Johnson et al. 1976, Osterkamp and Hupp 2010), and community trajectories can be interrupted and superimposed by new disturbances. Nevertheless, riparian disturbance regimes present an excellent opportunity to study succession at local scale. Frequent flood disturbance and the close proximity of forest stands that have colonized floodplain surfaces of different ages allow the use of chronosequences, or space-for-time proxies, to study successional processes in riparian communities (Stella et al. in review, Schnitzler 1995, Scott et al. 1997, Fierke and Kauffman 2005). In the absence of long-term longitudinal datasets, which with few exceptions are virtually absent for riparian areas (but see the case of the Missouri River, USA in Johnson et al. 2012), this approach is particularly suited to understand how community dynamics along highly modified rivers may diverge from historical or reference conditions (Prach and Walker 2011).

To date, the effect of human induced-modifications on riparian communities have mostly been studied by adopting a comparative approach. By comparing channelized versus unchannelized rivers (Dufour, Barsoum, Muller, & Piégay, 2007; Nakamura, Jitsu, Kameyama, & Mizugaki, 2002; Oswalt & King, 2005) or regulated versus unregulated rivers (Merritt and Cooper 2000, Kui et al. 2017, Bejarano et al. 2018), negative impacts to riparian communities have been documented, including reduced native species and functional trait diversity, increased invasion by exotic species, and homogenised forest stand structure. Despite widespread degradation to riparian systems and the substantial investigations into the ecological mechanisms that drive succession (Chang and Turner 2019), few studies have examined how modifications to river flow and sediment regimes impact the successional trajectory of riparian plant communities, and none to our knowledge have analysed these patterns in terms of functional trait dynamics. Yet, understanding both the current status and future trajectory of degraded riparian forest ecosystems is critical for defining and prioritizing effective strategies to conserve and restore them.

In this context, we aimed to understand how the current ecological trajectory of riparian forests along a large, channelized and regulated river in eastern France either paralleled or deviated from a relatively unmodified local reference system, across a range of successional phases. Using datasets of abiotic drivers – flow and sediment regimes – and biotic responses that included functional, structural and compositional attributes, we modeled chronosequences on both rivers to test for deviation in their ecological trajectories. The chronosequence approach is well-suited for assessing community shifts during plant succession, especially

if these changes are predictable over time (Walker et al. 2010). Moreover, comparing trends in species and trait composition over time can help to identify the mechanisms causing divergence in ecological trajectories, and thus potential barriers to restoration (Suding 2011, Chang and Turner 2019). Based on this scheme we addressed the following two questions: (i) How do abiotic and biotic conditions vary with forest stand age along a heavily impacted river compared to a more natural reference ecosystem? (ii) Are successional trajectories of riparian forests different between both river systems, in terms of species composition and functional trait trends over a long chronosequence?

Materials and methods

Study area

The study was carried out along the mainstem Rhône River (total length = 810 km, catchment area = 96,500 km², mean annual discharge = 1,700 $m^3 s^{-1}$) and the Drôme River (total length = 110 km, catchment area = 1,663 km², mean annual discharge = 20 $m^3 s^{-1}$), a tributary of the Rhône (Figure 1). Both rivers are located in SE France and experience a temperate climate with mean annual temperature and precipitation of 13.6°C and 755 mm in the southern part and of 11.9°C and 782 mm in the northern part. Despite differences in catchment size and discharge magnitude, the rivers prior to human modification shared similar snowmelt flow regimes and sediment dynamics. The riparian forests of both rivers contain a mix of early successional trees including *Populus nigra* and *Salix alba*, post-pioneers such as *Fraxinus excelsior* and *Acer platanoides*, and understorey species including *Crataegus monogyna and Sambucus nigra*. The most abundant newcomers to the species pool include the non-native trees *Acer negundo* and *Robinia pseudoacacia* (See Appendix S1 for further details on tree species' characteristics).

The Drôme River is a free-flowing river with a channel mostly unconstrained by human infrastructure and a shifting braided pattern throughout its downstream portion, which constitutes the study reach. Bedload is still actively transported in the lower section despite channel incision due to sediment mining that occurred during the 1970s. Since the second half of the 20th century, the Drôme River has also been subject to land-use changes in the floodplain (Liébault and Piégay 2002). Both mining and land-use changes have favored establishment of native riparian woodlands within the braided section, which is subject to periodic floods that scour older forest patches and induce sediment deposition and subsequent initiation of new stands. As a

consequence, the riparian forest is characterized by a complex mosaic of patches of different ages (Räpple et al. 2017).

The lower Rhône River, downstream of the city of Lyon, is a highly modified river, which has shifted from a braided pattern to a series of impounded reaches within the span of approximatively one century (Olivier et al. 2009, Bravard 2010). Two main historical management phases have greatly modified the river during this period. During the 19th Century the river was engineered and channelized of longitudinal submersible dikes and lateral dikes, forming more or less rectangular compartments, called "casiers Girardon" (see 1954 photo in Figure 1). These structures were constructed within the river's main channel and arranged sequentially along extensive reaches of the river to concentrate flow into a single narrow channel, thus facilitating navigation (see Thorel et al. 2018 for further details). In the second management phase, nineteen hydropower plants were built along the French part of the Rhône River during the second half of the 20th Century, among which sixteen plants were built on artificial channels that bypass 162 km out of 522 km of the river (Lamouroux et al. 2015). Each of these hydropower works contains a diversion dam that impounds a reservoir upstream and conveys a large part of the river discharge into the diversion canal on which the power plant is located for energy production (for further details see, Appendix S2 and Vázquez-Tarrío et al. 2019). As a consequence, the historical bypassed channels, also called the old Rhône, receives a minimum discharge most of the year, on average 5% of the natural discharge (Bravard and Gaydou 2015). Thus, these bypassed channels which had been previously channelized are also significantly impacted by river regulation, which have induce channel incision, lateral stabilization and armouring of the channel bed. Along the highly artificial, stable river margins of the bypassed channels, many of the Girardon structures filled with overbank fine sediment and were subsequently colonized by woody pioneer species and succeeded to mature riparian forests (Räpple 2018).

Riparian forest inventory sampling design

Forest inventories were conducted along both the Drôme and Rhône rivers and confined to established stands in the active and abandoned floodplain of each river. To ensure independence and avoid edge influences, all inventory plots were established > 60 m away from any other plot, were located in forested patches > 0.5 ha and were > 20 m from the nearest stand edge. Along the Drôme River, 69 plots were sampled in the summer of 1994 within the Natural Reserve of the Ramières, in which large patches of riparian forest remain. The plots were distributed between two braided reaches, west (n = 19 plots) and east (n = 50)

(Appendix S3). Along the Rhône River, 65 plots were surveyed along four bypassed channels (*i.e.*, the former active channel) in summer 2015. From upstream to downstream, these reaches were: Pierre-Bénite (PBN, n = 16 plots), Péage de Roussillon (PDR, n = 14), Montélimar (MON, n = 18) and Donzère-Mondragon (DZM, n = 17) (Appendix S3). Currently, the Girardon structures in these four bypassed channels support the largest extent of riparian forests remaining along the lower Rhône River downstream of Lyon.

On the Drôme River, stands were characterized using a 13.8-m-radius circular plot (area: 597 m²), centered on a systematic 130 x 130 m grid covering the whole forest area of the Natural Reserve. Within each plot, all standing trees with a diameter at breast height (DBH) ≥ 7.5 cm were recorded. On the Rhône River, a stratified sampling scheme was implemented, with plots randomly located within floodplain areas of known age. Rhône inventories used two concentric plot sizes, with a 10-m radius plot (area: 314 m²) for recording standing trees with a DBH ≥ 7.5 cm, and a larger plot of 20-m radius (area: 1,256 m²) used to record standing trees with DBH ≥ 30 cm. For each tree, species, DBH and health class were recorded, comprising live trees (< 50% dead crown and branches), dying trees (>50% dead crown and branches), or dead trees.

To accurately compare stand attributes between the two rivers, which were subject to different forest inventory campaigns, data were standardized to a per hectare basis and common metrics in both systems describing riparian forest composition and structure were used (Table 1). Basal area ($m^2\ ha^{-1}$), mean diameter (cm) and stem density ($n\ ha^{-1}$) were calculated for total live and total dead standing trees, as well as subsets for total exotic trees, and standing live trees of several genera: *Populus* spp. (i.e., *P. alba*, *P. x canescens*, *P. nigra*, *P. tremula* and *P. x canadensis*), *Fraxinus* spp. (i.e., *F. angustifolia* and *F. excelsior*) and *Acer* spp. (i.e., *A. campestre*, *A. monspessulanum*, *A. negundo*, *A. opalus*, *A. platanoides* and *A. pseudoplatanus*). Diversity metrics of tree diameter classes (5-cm ranges across n = 14 classes) and tree species (n = 31) were computed using the Shannon diversity index with integer values of basal area as the abundance weighting measure.

Overbank fine sediment depth was measured at the center of each plot using a soil corer that was inserted into the fine sediment until the gravel interface was reached (Table 1). Mean and standard-deviation of annual flow were calculated using daily data recorded between 1966 and 2017 for the Drôme River (http://hydro.eaufrance.fr) and between 1920 and 2010 for the Rhône River (provided by the Compagnie Nationale du Rhône). Because forest inventories on the two rivers were conducted in different periods (i.e., Drôme = 1994, Rhône = 2015), we used a common time frame, fixed between 1940 and 2000, to compare changes in hydrology but also to account for different switch-on dates of the diversion canals along the Rhône

River (i.e., DZM = 1952, MON = 1957, PBN = 1966, PDR = 1977). We used data from the Saillans measurement station on the Drôme River, 15 km upstream of the east sampling area, and from two stations on Rhône River, at Ternay within the PBN bypassed channel, and at Viviers within the MON bypassed channel. These two stations' data were then averaged to estimate unregulated flow prior to the diversions in each reach, whereas regulated flow levels were estimated using dam operation rules imposed following the diversions.

Trait data

Exotic tree species were distinguished from native tree species, using data available from the Baseflor database (Julve 1998). For functional traits, we focused on three traits that typically vary across different life history strategies as plants response to shifts in limiting resources and competitors during ecological succession: specific leaf area (SLA; leaf area per dry mass), wood density, and dry seed mass. SLA is related to resource acquisition and conservation strategies, contrasting "conservative" species with long-lived leaves to "acquisitive" species with rapid turnover of plant leaves (Wright et al. 2004). Wood density is related to growth strategy, contrasting fast-growing species with low wood density against slow-growing but stress-tolerant species with high wood density (Chave et al. 2009). Seed mass is related to dispersal ability, contrasting species with light seeds but high seedling mortality from species with large seeds but high long-term seedling survival (Westoby 1998). In riparian environments, where large and rapid changes in abiotic stressors and available resources drive community dynamics, this set of traits is expected to vary greatly among tree species and with forest stand age. Due to contrasting life-history strategies between pioneer and post-pioneer riparian species, we expected to see increasing trends across young to old forest stands in community weighted averages of SLA (from rapid to longer leaf turnover), wood density (from faster to slower growth) and seed mass (from long-distance to more local dispersal).

Trait data were extracted from the TRY database, from which we calculated a mean trait value per species, after removing all values with an error risk > 4 (Kattge et al. 2011, see Appendix S4). Missing values in the wood density data were completed using the global wood density database (Zanne et al. 2009, Chave et al. 2009). For each trait value, we computed community-weighted means (CWM) and functional dispersion (FDis) using basal area as a measure of relative abundance. CWM is defined as the mean of trait values weighted by the relative abundance of each species bearing each value (Lavorel et al. 2008). FDis is defined as the mean distance of individual species to the weighted centroid of all species in the assemblage and is unaffected by difference in species richness among plots (Laliberté and Legendre, 2010).

Forest stand age reconstruction

Forest stand age was characterized using geo-referenced aerial photograph series in a Geographic Information System (QGIS Development Team 2015). For the Drôme River, seven series of aerial photographs were available, taken from 1932 to 1991. For the Rhône River, available information varied among reaches and among plot positions within reach, with four to six series of aerial photographs available per reach, taken from 1938 to 2002 (see Appendix S3 for details). For each plot, the physiognomic unit was characterized visually from aerial photographs into four categories: water, bare ground, shrub (*i.e.,* sparse patches of low vegetation) and forest units (*i.e.,* dense patches of tall vegetation). The effective timing of forest establishment for each plot was determined by averaging the last unforested series date (t = no forest cover) and the next one where forest was evident (t+x = forest cover). When a time-series was too fragmented, i.e., > 20 years between two superimposed aerial photographs, and when physiognomic units were "shrub" on the old aerial photograph series and "forest" on the next series, the date of forest cover was approximated in between the two dates. To confirm the continuity of the forest cover since the first date of appearance, posterior aerial photograph series were also inspected (Appendix S3).

Statistical analysis

We used linear models to test how abiotic drivers and biotic responses varied across the forest stand age (or years), and whether these trends differed significantly between rivers. For all models, we considered forest stand age ("Age" in tables and figures) as a continuous predictor, as well as sediment depth ("Sed_depth"). Both of these variables were standardized prior to analysis. River (noted "River") was considered as an independent, categorical factor. Abiotic drivers included the fine sediment depth as well as the mean and standard deviation (SD) of annual flow. Because the discharge was largely different between the two rivers, mean and SD of annual flow were standardized according to the range of their own values prior to analysis. Biotic response included the community-weighted mean (CWM) and the dispersion (FDis) of functional trait values, the basal area, the mean diameter and the stem density of stand attributes and of tree genera as well as the diversity indices (Table 1). Because the seed mass of two tree species – *Juglans regia* and *Quercus pubescens* – was very large, seed mass values were log-transformed before CWM and FDis calculation.

To investigate how abiotic drivers and biotic responses varied over time between the two rivers, we fitted normal linear models (LMs) or log-normal LMs for skewed response variables (i.e., sediment depth, SLA, wood density, basal area, diameter and stem density). We developed a set of *a priori* models testing the

252 individual, additive and interactive effects of predictor variables, plus a null (*i.e.,* intercept-only) model (see
253 Appendices S5 and S6). In all candidate models the variance inflation factor was < 3. The most parsimonious
254 model was identified using Akaike's information criterion corrected for small sample sizes (Burnham and
255 Anderson 2002) and goodness of fit was estimated using the adjusted coefficient of determination. For all of
256 the response variables, Moran's I values in the top-ranked model residuals was non-significant, indicating that
257 spatial patterns were accounted for by independent variables (Appendix S7). For each response variable,
258 parameter estimates and associated unconditional standard errors were extracted from the top-ranked model
259 and we checked for consistency among parameter estimates and confidence intervals on the subset of top
260 ranking models for which the delta AICc was < 7 (Appendix S5 and S6).
261 To investigate whether the forest structure and composition varied with forest stand age between the
262 two rivers we used multivariate generalized linear models (GLMs). We fitted the full model (Age x River +
263 Sed_depth) to each diameter class/tree species, using basal area as the abundance measure, and summed
264 across the univariate responses to estimate their multivariate response with a negative binomial distribution.
265 The significance of independent variables in the multivariate GLM was assessed using an analysis of variance
266 with the PIT-trap method and 999 bootstrap resamples (Warton et al. 2017). To determine which diameter
267 classes/tree species best contribute to the overall model deviation, we calculated univariate test statistics and
268 p-values, and adjusted to correct for multiple testing for each diameter classes and tree species (Wang et al.
269 2012). Finally, to provide a graphical representation of the interaction between forest stand age and river, we
270 used a canonical analysis of principal coordinates (Anderson and Willis 2003), using a Bray-Curtis distance. All
271 analyses were performed with R version 3.5.3. (R Core Team 2019).
272
273 **Results**
274 **Contrasting trends in abiotic drivers among rivers**
275 Of the abiotic drivers analysed, sediment depth and mean annual flow had pronounced trends over
276 time that differed significantly between the Rhône and Drôme rivers (Table 2; Figure 2). Thus, models that
277 included an interaction term between river and forest stand age (for sediment depth) or river and year (for
278 mean discharge) best predicted the respective response. Sediment depth increased more rapidly with forest
279 stand age along the Rhône compared to the Drôme (Figure 2), whereas the mean annual flow strongly
280 decreased over time along the Rhône, with no clear trend on the Drôme (Appendix S8). The standard-deviation

281 of annual flow decreased significantly over time (Figure 2) but did not differ significantly between the two
282 rivers (Appendix S8).

283 **Trends in forest functional, structural and compositional attributes**

284 Most of the whole-stand and genera-specific forest attributes, community-weighted functional traits,
285 and diversity indices varied strongly with riparian forest stand age. Similar to the abiotic drivers, many of the
286 trends in forest development also differed significantly between rivers. For a large fraction of the response
287 variables, the top-ranked model included the interaction term between stand age and river, and some of these
288 included sediment depth as a covariate (Table 2). The goodness of fit of these models ranged greatly, from 0.08
289 for the basal area of *Populus spp*., to 0.71 for the mean diameter of *Populus* spp. (Table 2).

290 Parameters retained in the top ranked models indicate that only a few trends in forest characteristics
291 were equivalent between rivers; these were overall mean seed mass, and for *Fraxinus* spp. only, their basal
292 area and stem density (Table 3). Some characteristics varied at the same rate (i.e., parallel slopes for both
293 rivers), but differed significantly in magnitude between the Drôme and Rhône. These included stem density for
294 live and dead trees, which were consistently higher along the Drôme River. In contrast, stem density and mean
295 tree diameter for exotic trees, mean tree diameter for *Fraxinus* spp. and *Acer* spp., as well as functional
296 dispersion of SLA were significantly higher along the Rhône River (Table 1; Figure 3 and 4).

297 All others trait and stand-level responses were mediated by the interaction terms between river and
298 forest stand age (Tables 3). For example, the mean value for SLA and wood density (Figure 3), and the basal
299 area of exotic trees (Figure 4) increased more steeply with forest stand age along the Rhône River. Conversely,
300 the Drôme River riparian forest showed steeper trends over time for the trait dispersion of wood density and
301 seed mass (Figure 3), *Acer* spp. basal area and stem density (Figure 5), as well as the diversity of tree species
302 and of stem diameter classes (Figure 6). For some responses, the two rivers showed opposite trends. In
303 particular, the basal area and mean diameter of live and dead trees (Figure 4), as well as the basal area of
304 native *Populus spp*. (Figure 5), increased with forest stand age along the Drôme River but, counter to most
305 patterns of stand development, decreased along the Rhône River. The mean diameter of *Populus* trees was
306 much larger along the Rhône, and they achieved their maximum size much faster, within two decades (Figure
307 5). This, combined with the decreasing density of these large, dominant trees later in the successional
308 sequence had the effect of lowering *Populus* and overall stand basal area with time, in contrast to the Drôme,
309 where both metrics increased.

310 Finally, sediment depth was a significant predictor for all stand basal area fractions (live, dead, and
311 exotic trees), for *Fraxinus* density, and for *Acer spp*. basal area, mean diameter and density. However, the
312 effect of sediment was positive for *Acer* spp. basal area and density but negative for *Fraxinus* spp. density and
313 *Acer* spp. mean diameter (Table 3).

314 **Differences in forest composition and structure between rivers**

315 The multivariate GLMs showed that forest structure was significantly influenced by forest stand age
316 (Dev = 14.5, $P = 0.031$), river (Dev = 73.8, $P = 0.001$), sediment depth (Dev = 22.3, $P = 0.034$) and the interaction
317 term between age and river (Dev = 20.7, $P = 0.043$). Based on the deviation explained by parameters, most of
318 the variation in forest structure was related to differences between rivers; this dichotomy is well-represented
319 by the separation of Rhône and Drôme plots along the first axis of the canonical analysis of principal
320 coordinates (CAP 1, Figure 7A). The second axis was more evidently related to forest age, though some sites
321 appeared to be well outside the predominant distribution. Univariate tests for each diameter class showed that
322 the largest trees (DBH > 70 cm) had the highest test statistic values for the effect size between rivers (Dev =
323 25.15, $P_{adj} < 0.001$) (Appendix S9). Consequently, divergence in forest structure between the two rivers was
324 mostly due to the greatest abundance of very large diameter trees within the Rhône River forests (mean basal
325 area/plot = 8.17 $m^2\ ha^{-1}$) as compared to the Drôme River (mean basal area/plot = 0.11 $m^2\ ha^{-1}$).

326 As with forest structure, community composition was significantly influenced by river (Dev = 340.7, $P =$
327 0.001) and the interaction term between age and river (Dev = 49.6, $P = 0.040$); this is similarly evident in the
328 plot clustering along the first CAP axis (Figure 7B). However, community composition was much less influenced
329 than forest structure by stand age (Dev = 40.2, $P = 0.063$) and sediment depth (Dev = 33.2, $P = 0.437$). The CAP
330 plot shows that age classes were quite dispersed and randomly distributed along the second axis. Furthermore,
331 the Drôme River plots were more clustered than the Rhône River plots, indicating greater similarity in tree
332 species composition within the Drôme River corridor compared to the Rhône. Univariate tests for each tree
333 species showed that *Acer negundo* has the largest effect size between the rivers (Dev = 130.30, $P_{adj} < 0.001$)
334 (Appendix S10). Consequently, divergence in forest composition between the two rivers was in large part due
335 to the absence of this exotic species within the Drôme River forests (mean plot basal area = 0.00 $m^2\ ha^{-1}$) as
336 compared to the Rhône River (mean plot basal area = 5.37 $m^2\ ha^{-1}$).

337

338 **Discussion**

Overall, the successional trajectories of riparian forests along the channelized and regulated bypassed channels of the Rhône River deviate from the expected historical trajectories, as represented by the unchannelized and unregulated reaches of the Drôme River . Though the riparian forests of the Drôme River are also under the influence of multiple human-induced stressors (Liébault and Piégay 2002), and though many trends in species composition and community functional traits followed expected forest stand trajectories, differences between the two rivers were stronger than the age gradient, which spanned 70 years in this study. Because the biogeographic setting and potential species pools are similar, these results strongly suggest that large differences in local environmental conditions are driving riparian forest development patterns (Clark et al. 2019). Many of the shifts along the Rhône River chronosequence were more pronounced and rapid compared to the Drôme, in particular for foundation species (e.g., *Populus* spp.) and invasive exotic species (e.g., *Acer negundo*) (Figure 8). In light of these rapid and profound divergences in community composition and structure, mostly related to cumulative effect of human-induced stressors, it may be argued that the resulting riparian forests correspond to the definition of a "novel ecosystem" (Hobbs et al. 2009). Indeed, the riparian forests of Rhône River are rapidly dominated by non-native species, and the greatly supressed disturbance regime (Vázquez-Tarrío et al. 2019) and lack of pioneer forest regeneration along bypassed channels, impedes community dynamics processes evident in more natural reference systems (e.g., Stella et al. in review, Fierke and Kauffman 2005, Balian and Naiman 2005). In this severely degraded system, it therefore seems more pragmatic to prioritize management and restoration measures toward desired human benefits rather than target a return to a potential reference state (Dufour and Piégay 2009).

Flow regulation and channelization induce rapid changes in abiotic conditions

Strongly divergent trends in abiotic conditions were evident between the two river systems. While it cannot be ruled out that natural differences in physical and ecological conditions between the Drôme and the Rhône watersheds could be a driver behind this observed effect, we inferred that the different management histories of the Rhône and Drôme is one of the most important ecological drivers. Along the highly artificial, stable river margins of the Rhône River, the Girardon dike structures were very effective in trapping suspended sediment, with very high accumulation rates of overbank fine sediment, especially immediately after the initial channelization and prior to the dam construction period (for further details see, Tena et al. 2020). Large quantities of fine sediment trapped along channelized river margins have been shown to increase ecosystem productivity by maintaining higher nutrient pools (Franklin et al. 2009). In addition, high overbank

368 sedimentation rates induce strong differences in soil properties (e.g., texture and moisture retention), which
369 can also promote a resource-rich environment. These factors may explain the rapid and vigorous growth of
370 pioneer trees, particularly *Populus* species that reached maximum tree sizes very quickly, i.e., at a very early
371 stage in the succession sequence. Overall, the increase in bank accretion, the decrease in overbank flows
372 (Figure 2) as well as the lowering of the water table due to river entrenchment, has induced gradual
373 disconnection between the channelized margins and the main channel. This has ultimately led to changes in
374 channel morphology and physical conditions on the Rhône, i.e., a shift from anabranching reaches to narrow,
375 very stable, single thread channels (Tena et al. 2020), as has been shown on other rivers (Wilcock and Essery
376 1991, Marston et al. 1995).
377 Disconnection of the riparian zone from the river channel is even more exacerbated by changes in the
378 hydrologic regime, as evidenced by the decrease in the mean annual flow along the Rhône River since the
379 1940s. This decrease is mainly due to water diversion into lateral canals following the construction of multiple
380 hydropower dams in the post-war period, which were commissioned at different dates along the Rhône
381 corridor (i.e., DZM = 1952, MON = 1957, PBN = 1966, PDR = 1977, see also Figure 2). The combined effects of
382 high overbank sedimentation rates and pronounced decreases in the mean annual discharge induced a loss of
383 up to 60% of the active channel surface of the Rhône River (Tena et al. 2020). Tena et al. (2020) found that
384 along the bypassed channels the terrestrialization process and associated vegetation encroachment were
385 primarily driven by the Girardon dike structures (i.e., channelization) rather than by flow regulation. The
386 cumulative effects of channel correction and regulation can also induce a rapid decline in the groundwater
387 table and thus a more limited access to soil water for existing riparian trees (Franklin et al. 2009), which on the
388 Rhône River may have been amplified locally by gravel extraction and pumping for irrigation (Thorel et al.
389 2018). Finally, channelization and flow regulation may reduce the variability of hydrologic conditions, especially
390 lower intensity and frequency of flooding on higher riparian floodplains, as well as bedload transport capacities
391 (Vázquez-Tarrío et al. 2019). Conversely, along the Drôme River, low rate of fine sediment accumulation and
392 maintenance of a natural flow regime likely promote a dynamic equilibrium across successional phases without
393 the rapid change in floodplain conditions that both correction and regulation induced on the Rhône (Figure 8).
394 Overall, our results pointed out profound changes in hydro-geomorphic processes between the two river
395 systems. In this view, we suggest that the artificially stabilizing effect of the combined Girardon structures and

flow regulation on the Rhône River enabled the development of a distinct and potentially unique riparian forest community (Thorel et al. 2018).

Changes in abiotic conditions strongly alter the functional, structural and compositional attributes of riparian forests

Consistent with changes in abiotic conditions over time, our results demonstrate rapid divergence in riparian forest dynamics between the two river systems, reflecting environmental selection toward a pool of traits and species best adapted to local conditions (Figure 8). Although successional shifts in plant functional traits followed predictable successional trajectories along both rivers, (e.g., Fierke and Kauffman 2005, Van Pelt et al. 2006, Muñoz-Mas et al. 2017), increases in wood density and SLA values within the riparian forest were faster along the Rhône River (Figure 3). Specifically, our results show that channelization and flow regulation accelerate the transition from a disturbance-dependent pioneer community, i.e., fast-growing tree species with high resource acquisition strategies, to a post-pioneer community dominated by slow-growing, competitive species with high resource conservation and retention strategies (Marston et al. 1995, Oswalt and King 2005). This accelerated shift in plant ecological strategy is likely related to both a more limited access to groundwater and high overbank sedimentation rates promoting resource-rich environments along the Rhône, both of which were mediated by changes to the hydrologic and disturbance regimes (Figure 2) (see also, Vázquez-Tarrío et al. 2019). Consequently, there has been a major divergence in plant habitat niches between the two river systems, and large corresponding differences in stand attributes (Figure 4), plant assemblages (Figure 7) and forest successional pathways. These results reinforce the importance of contingent factors in determining ecological trajectories, as has been shown for old fields and other successional contexts (e.g., Clark et al. 2019)

Prolonged and rapid decline in the groundwater table has been shown to greatly alter growth and survival of pioneer species requiring permanent access to soil water (Reily and Johnson 1982, Scott et al. 1999, Lite and Stromberg 2005, Stella et al. 2013a), and favor more competitive species such as post-pioneer and exotic species (Merritt and Poff 2010, González et al. 2010, Nadal-Sala et al. 2017). Within the region encompassed by our study, radial growth of *Populus nigra* , an obligate phreatophyte that dominates early successional forest stands, is more sensitive to groundwater manipulation compared to the mesophytic species *Fraxinus excelsior*, which can use both soil moisture and deeper groundwater opportunistically to maintain more constant inter-annual growth (Singer et al. 2013). Relative basal area and mean diameter of post-pioneer species, including *Fraxinus* spp. and *Acer* spp., increased over time in both rivers. For *Populus* species, however,

while tree diameter and stem density varied consistently between the two rivers, the basal area increased along the Drôme but decreased along the Rhône. In addition, most of the divergence in species composition between the two river systems was due to the great abundance of the exotic invasive species *Acer negundo* along the Rhône River. Compared to native pioneer and post-pioneer tree species, *Acer negundo* shows higher level of plasticity in foliage allocation (i.e., larger specific leaf area and total leaf area) when resources are not limiting, thus allowing for better growth and survival (Porté et al. 2011). Thus, the temporal trends in whole-stand (Figure 4) and genus-specific (Figure 5) tree distributions suggest that channelization and flow regulation have promoted a resource-rich environment within the Girardon structures (Tena et al. 2020), leading to an acceleration of ecological succession due to faster growth and mortality of native pioneer species and to better survival and establishment of stress tolerant species, including exotic species (Catford et al. 2014).

Resource-rich environments also benefit native species, in particular high growth rates of *Salicaceae* species (Karrenberg et al. 2002) and other, more competitive species (e.g., Porté et al. 2011, Nadal-Sala et al. 2017). The Rhône River experienced much faster biomass accumulation, mostly due to the greater abundance of very large trees that achieved their maximum size within 20 years. Contrary to expectations, however, basal area and mean tree diameter of both live and dead fractions decreased with stand age along the Rhône River. The anomalous pattern on the Rhône was mostly due to the scarcity of very large pioneer trees (primarily *Salix* spp. and *Populus* spp.) in mature forest stands. Though they are generally short-lived trees, their rapid reduction in density along the Rhône meant that overall basal area decreased on that river with forest age, whereas it continued to increase on the Drôme, as expected. Since biomass usually increases along the initial successional phases in riparian forests (e.g., Fierke and Kauffman 2005, Balian and Naiman 2005, Van Pelt et al. 2006), even along regulated rivers (Stella et al. in review), these results suggest that several interacting stressors may be responsible for the unusual patterns. One explanation may be the rapid dewatering and hydric stress that followed flow reductions in the bypassed channels with the operation of the post-war hydropower canals. This would have preferentially affected older, established trees that could not adjust to the new groundwater regime, increasing mortality of pioneer trees and reducing the growth rate of survivors in the oldest stands. Another potential factor is selective cutting of larger trees along levees and dikes, which was sometimes conducted by farmers and/or river managers of the “Compagnie Nationale du Rhône” in order to protect the structural integrity of dikes and limit large wood inputs to the main channel. As such, patterns observed along the Rhône River most likely result from cumulative multiple stressors related to human activity,

mainly channelization and flow regulation but also occasionally selective cutting, which are difficult to disentangle from other drivers (Stella and Bendix 2018).

The increase in trait dispersion over time (Figure 3) indicates that older floodplain forests increasingly support co-occurring species with contrasting ecological strategies (Figure 3). Hydro-geomorphic changes over time not only drive changes in abiotic conditions at the floodplain scale but may also induce greater habitat heterogeneity at finer scale, potentially due to greater variability in topographic and hydrologic conditions. Accordingly, several authors have reported an increase in tree species richness with later successional stages in riparian forests (Schnitzler 1995, Nakamura et al. 1997, Van Pelt et al. 2006). Here, we showed that ecological succession in riparian forests not only promotes taxonomic diversity (Figure 6) but also functional diversity (Figure 3). The contrasts in functional traits between rivers suggest that the riparian forests of the Rhône River underwent a more rapid change to functionally different species assemblages compared to the Drôme. Indeed, our results show that the shift in community-weighted SLA and wood density was accelerated along the Rhône River (Figure 3). In contrast, the trait dispersion for seed mass was more pronounced along the Drôme River, indicating a higher occurrence of tree species with small seed mass (i.e., mostly *Salicaceae*) in older stands. Given the importance of floods and hydrochory in maintaining early successional forest stands (Scott et al. 1997, Fraaije et al. 2017), the greater representation of pioneer species within more successional stages on the Drôme River further confirms the influence of dynamic fluvial processes (e.g., flooding, channel migration) in riparian successional processes on intact rivers, compared to a stabilized and controlled environment as on the Rhône .

Conclusion

In comparing successional trajectories between the heavily modified Rhône and more natural Drôme rivers, we found that the legacy of cumulative impacts of river channelization and flow regulation strongly altered the structure, composition and ecological trajectory of riparian forests. These findings accord with prior studies along heavily modified rivers (Merritt and Cooper 2000, Nakamura et al. 2002, Oswalt and King 2005, Dufour et al. 2007, González et al. 2010, Johnson et al. 2012). By using a chronosequence modelling approach, we illustrated the parallel changes in river conditions, riparian forest structure and composition, and functional trait expression within the plant community along a successional gradient. Thus, although the earliest phase of stand development (< 20 years) on both rivers was characterized by the dominance of pioneer and

disturbance-dependent species, the shift to a mature forest stage dominated by post-pioneer and exotic species was greatly accelerated (within 20-50 years) along the Rhône River (Figure 8). Beyond differences not related to human-induced stressors, this accelerated shift was likely linked to the fact that the Rhône River margins have experienced a more rapid terrestrialization than natural floodplains, due to the combined effect of less frequent and lower magnitude flooding events, greater overbank fine sediment deposition, and a decline in groundwater tables due to flow diversion. Thus, by disrupting natural hydro-geomorphological processes at different spatial and temporal scales, channelization and flow regulation have induced severe and long-term changes in environmental conditions, in turn driving riparian plant communities far from their historical reference trajectories (Figure 7). Due to the strong differences in the biotic community, as well as their abiotic drivers, we suggest that restoration of the Rhône River riparian forests to a more natural (i.e., pre-development) state is highly improbable, even if physical conditions such as flooding and bank revetment are mitigated by restoration actions. The novel structural, compositional and functional attributes of the Rhône riparian forest, including the dominance of non-native species in the regeneration fraction and understory, suggest that the forest will be highly resistant to change and that process-based restoration actions would likely have a long and persistent hysteresis (Suding et al. 2004). In this system as in other severely degraded ones, riparian management may benefit from a more pragmatic approach focusing on desired human benefits (Dufour and Piégay 2009) and specific ecological targets (Palmer et al. 2005). For the Rhône River's riparian forest, which is increasingly valued for its ecological and cultural legacy, these approaches may include active stand management by selective cutting to remove exotic species and enhance native tree diversity, promoting through active and passive means and pioneer stages which are no longer rejuvenated, as well as enhancing other ecosystem services such as flood and pollutant mitigation, carbon storage, and habitat quality for wildlife and fish.

Authors' contributions

P.J., J.C.S., H.P. and A.E. conceived and designed the experiments. J.C.S., B.R., P.B., J-M.F. and C.J. collected the data. P.J. analysed the data and wrote the first draft of the manuscript. All authors contributed critically to the drafts and gave final approval for publication.

Acknowledgements

512 The study has been supported by the TRY initiative on plant traits (http://www.try-db.org). The TRY initiative
513 and database is hosted, developed and maintained by J. Kattge and G. Boenisch (Max Planck Institute for
514 Biogeochemistry, Jena, Germany). TRY is currently supported by Future Earth/bioDISCOVERY and the German
515 Center for Integrative Biodiversity Research (iDiv) Halle-Jena-Leipzig. This work was cofunded by the Labex
516 DRIIHM, which is managed by the ANR, French program "Investissements d'Avenir" (ANR-11-LABX-0010), the
517 OHM Vallée du Rhône and IRSTEA. It was also performed within the framework of the EUR H2O'Lyon (ANR-17-
518 EURE-0018) of Université de Lyon (UdL).
519
520 **References**
521 Anderson, M. J., and T. J. Willis. 2003. Canonical analysis of principal coordinates: a useful method of
522 constrained ordination for ecology. Ecology 84:511–525.
523 Balian, E. V., and R. J. Naiman. 2005. Abundance and production of riparian trees in the lowland floodplain of
524 the Queets River, Washington. Ecosystems 8:841–861.
525 Beisner, B., D. Haydon, and K. Cuddington. 2003. Alternative stable states in ecology. Frontiers in Ecology and
526 the Environment 1:376–382.
527 Bejarano, M. D., C. Nilsson, and F. C. Aguiar. 2018. Riparian plant guilds become simpler and most likely fewer
528 following flow regulation. Journal of Applied Ecology 55:365–376.
529 Bendix, J., and J. C. Stella. 2013. Riparian vegetation and the fluvial environment: a biogeographic perspective.
530 Pages 53–74 *in* D. Butler and C. Hupp, editors. Treatise on Geomorphology, Vol 12,
531 Ecogeomorphology. Elsevier.
532 Bravard, J.-P. 2010. Discontinuities in braided patterns: the River Rhône from Geneva to the Camargue delta
533 before river training. Geomorphology 117:219–233.
534 Bravard, J.-P., and P. Gaydou. 2015. Historical development and integrated management of the Rhône River
535 floodplain, from the Alps to the Camargue delta, France. Pages 289–320 *in* P. F. Hudson and H.
536 Middelkoop, editors. Geomorphic approaches to integrated floodplain management of lowland fluvial
537 systems in North America and Europe. Springer New York, New York, NY.
538 Burnham, K. P., and D. R. Anderson. 2002. Model selection and multi-model inference: a practical information-
539 theoretic approach, 2nd ed. Springer-Verlag, New York.

Catford, J. A., W. K. Morris, P. A. Vesk, C. J. Gippel, and B. J. Downes. 2014. Species and environmental characteristics point to flow regulation and drought as drivers of riparian plant invasion. Diversity and Distributions 20:1084–1096.

Chang, C. C., and B. L. Turner. 2019. Ecological succession in a changing world. Journal of Ecology 107:503–509.

Chave, J., D. Coomes, S. Jansen, S. L. Lewis, N. G. Swenson, and A. E. Zanne. 2009. Towards a worldwide wood economics spectrum. Ecology Letters 12:351–366.

Clark, A. T., J. M. H. Knops, and D. Tilman. 2019. Contingent factors explain average divergence in functional composition over 88 years of old field succession. Journal of Ecology 107:545–558.

Connell, J. H., and R. O. Slatyer. 1977. Mechanisms of succession in natural communities and their role in community stability and organization. The American Naturalist 111:1119–1144.

Dufour, S., N. Barsoum, E. Muller, and H. Piégay. 2007. Effects of channel confinement on pioneer woody vegetation structure, composition and diversity along the River Drôme (SE France). Earth Surface Processes and Landforms 32:1244–1256.

Dufour, S., and H. Piégay. 2009. From the myth of a lost paradise to targeted river restoration: forget natural references and focus on human benefits. River Research and Applications 25:568–581.

Fierke, M. K., and J. B. Kauffman. 2005. Structural dynamics of riparian forests along a black cottonwood successional gradient. Forest Ecology and Management 215:149–162.

Folke, C., S. Carpenter, B. Walker, M. Scheffer, T. Elmqvist, L. Gunderson, and C. S. Holling. 2004. Regime shifts, resilience, and biodiversity in ecosystem management. Annual Review of Ecology, Evolution, and Systematics 35:557–581.

Fraaije, R. G. A., S. Moinier, I. van Gogh, R. Timmers, J. J. van Deelen, J. T. A. Verhoeven, and M. B. Soons. 2017. Spatial patterns of water-dispersed seed deposition along stream riparian gradients. PLOS ONE 12:e0185247.

Franklin, S. B., J. A. Kupfer, S. R. Pezeshki, R. Gentry, and R. D. Smith. 2009. Complex effects of channelization and levee construction on western Tennessee floodplain forest function. Wetlands 29:451–464.

González, E., M. González-Sanchis, Á. Cabezas, F. A. Comín, and E. Muller. 2010. Recent changes in the riparian forest of a large regulated mediterranean River: implications for management. Environmental Management 45:669–681.

568 Hobbs, R. J., E. Higgs, and J. A. Harris. 2009. Novel ecosystems: implications for conservation and restoration.
569 Trends in Ecology & Evolution 24:599–605.
570 Johnson, W. C., R. L. Burgess, and W. R. Keammerer. 1976. Forest overstory vegetation and environment on the
571 Missouri River floodplain in North Dakota. Ecological Monographs 46:59–84.
572 Johnson, W. C., M. D. Dixon, M. L. Scott, L. Rabbe, G. Larson, M. Volke, and B. Werner. 2012. Forty years of
573 vegetation change on the Missouri River floodplain. BioScience 62:123–135.
574 Julve, P. 1998. Baseflor. Index botanique, écologique et chorologique de la flore de France. Version : 2017.
575 http://perso.wanadoo.fr/philippe.julve/catminat.htm.
576 Karrenberg, S., P. J. Edwards, and J. Kollmann. 2002. The life history of Salicaceae living in the active zone of
577 floodplains. Freshwater Biology 47:733–748.
578 Kattge, J., S. Díaz, S. Lavorel, I. C. Prentice, P. Leadley, G. Bönisch, E. Garnier, M. Westoby, P. B. Reich, I. J.
579 Wright, J. H. C. Cornelissen, C. Violle, S. P. Harrison, P. M. Van Bodegon, M. Reichstein, B. J. Enquist, N.
580 A. Soudzilovskaia, D. D. Ackerly, M. Anand, O. Atkin, M. Bahn, T. R. Baker, D. Baldocchi, R. Bekker, C. C.
581 Blanco, B. Blonder, W. J. Bond, R. Bradstock, D. E. Bunker, F. Casanoves, J. Cavender-Bares, J. Q.
582 Chambers, F. S. Chapin III, J. Chave, D. Coomes, W. K. Cornwell, J. M. Craine, B. H. Dobrin, L. Duarte, W.
583 Durka, J. Elser, G. Esser, M. Estiarte, W. F. Fagan, J. Fang, F. Fernández-Méndez, A. Fidelis, B. Finegan,
584 O. Flores, H. Ford, D. Frank, G. T. Freschet, N. M. Fyllas, R. V. Gallagher, W. A. Green, A. G. Gutierrez, T.
585 Hickler, S. I. Higgins, J. G. Hodgson, A. Jalili, S. Jansen, C. A. Joly, A. J. Kerkhoff, D. Kirkup, K. Kitajima, M.
586 Kleyer, S. Klotz, J. M. H. Knops, K. Kramer, I. Kühn, H. Kurokawa, D. Laughlin, T. D. Lee, M. Leishman, F.
587 Lens, T. Lenz, S. L. Lewis, J. Lloyd, J. Llusià, F. Louault, S. Ma, M. D. Mahecha, P. Manning, T. Massad, B.
588 E. Medlyn, J. Messier, A. T. Moles, S. C. Müller, K. Nadrowski, S. Naeem, U. Niinemets, S. Nöllert, A.
589 Nüske, R. Ogaya, J. Oleksyn, V. G. Onipchenko, Y. Onoda, J. Ordoñez, G. Overbeck, W. A. Ozinga, S.
590 Patiño, S. Paula, J. G. Pausas, J. Peñuelas, O. L. Phillips, V. Pillar, H. Poorter, L. Poorter, P. Poschlod, A.
591 Prinzing, R. Proulx, A. Rammig, S. Reinsch, B. Reu, L. Sack, B. Salgado-Negret, J. Sardans, S. Shiodera, B.
592 Shipley, A. Siefert, E. Sosinski, J.-F. Soussana, E. Swaine, N. Swenson, K. Thompson, P. Thornton, M.
593 Waldram, E. Weiher, M. White, S. White, S. J. Wright, B. Yguel, S. Zaehle, A. E. Zanne, and C. Wirth.
594 2011. TRY - a global database of plant traits. Global Change Biology 17:2905–2935.

595 Kui, L., J. C. Stella, P. B. Shafroth, P. K. House, and A. C. Wilcox. 2017. The long-term legacy of geomorphic and
596 riparian vegetation feedbacks on the dammed Bill Williams River, Arizona, USA. Ecohydrology
597 10:e1839.
598 Laliberté, E., and P. Legendre. 2010. A distance-based framework for measuring functional diversity from
599 multiple traits. Ecology 91:299–305.
600 Lamouroux, N., J. A. Gore, F. Lepori, and B. Statzner. 2015. The ecological restoration of large rivers needs
601 science-based, predictive tools meeting public expectations: an overview of the Rhône project.
602 Freshwater Biology 60:1069–1084.
603 Lavorel, S., K. Grigulis, S. McIntyre, N. S. G. Williams, D. Garden, J. Dorrough, S. Berman, F. Quétier, A. Thébault,
604 and A. Bonis. 2008. Assessing functional diversity in the field – methodology matters! Functional
605 Ecology 22:134–147.
606 Liébault, F., and H. Piégay. 2002. Causes of 20th century channel narrowing in mountain and piedmont rivers of
607 southeastern France. Earth Surface Processes and Landforms 27:425–444.
608 Lite, S. J., and J. C. Stromberg. 2005. Surface water and ground-water thresholds for maintaining Populus–Salix
609 forests, San Pedro River, Arizona. Biological Conservation 125:153–167.
610 Marston, R. A., J. Girel, G. Pautou, H. Piégay, J.-P. Bravard, and C. Arneson. 1995. Channel metamorphosis,
611 floodplain disturbance, and vegetation development: Ain River, France. Geomorphology 13:121–131.
612 Meiners, S. J., M. W. Cadotte, J. D. Fridley, S. T. A. Pickett, and L. R. Walker. 2015. Is successional research
613 nearing its climax? New approaches for understanding dynamic communities. Functional Ecology
614 29:154–164.
615 Merritt, D. M., and D. J. Cooper. 2000. Riparian vegetation and channel change in response to river regulation:
616 a comparative study of regulated and unregulated streams in the Green River basin, USA. Regulated
617 Rivers: Research and management 16:543–564.
618 Merritt, D. M., and N. L. R. Poff. 2010. Shifting dominance of riparian *Populus* and *Tamarix* along gradients of
619 flow alteration in western North American rivers. Ecological Applications 20:135–152.
620 Mouillot, D., N. A. J. Graham, S. Villéger, N. W. H. Mason, and D. R. Bellwood. 2013. A functional approach
621 reveals community responses to disturbances. Trends in Ecology & Evolution 28:167–177.
622 Muñoz-Mas, R., V. Garófano-Gómez, I. Andrés-Doménech, D. Corenblit, G. Egger, F. Francés, M. T. Ferreira, A.
623 García-Arias, E. Politti, R. Rivaes, P. M. Rodríguez-González, J. Steiger, F. J. Vallés-Morán, and F.

624 Martínez-Capel. 2017. Exploring the key drivers of riparian woodland successional pathways across
625 three European river reaches. Ecohydrology 10:e1888.
626 Nadal-Sala, D., S. Sabaté, E. Sánchez-Costa, S. Poblador, F. Sabater, and C. Gracia. 2017. Growth and water use
627 performance of four co-occurring riparian tree species in a Mediterranean riparian forest. Forest
628 Ecology and Management 396:132–142.
629 Naiman, R. J., and H. Decamps. 1997. The ecology of interfaces: riparian zones. Annual review of Ecology and
630 Systematics 28:621–658.
631 Nakamura, F., M. Jitsu, S. Kameyama, and S. Mizugaki. 2002. Changes in riparian forests in the Kushiro Mire,
632 Japan, associated with stream channelization. River Research and Applications 18:65–79.
633 Nakamura, F., T. Yajima, and S. Kikuchi. 1997. Structure and composition of riparian forests with special
634 reference to geomorphic site conditions along the Tokachi River, northern Japan. Plant Ecology
635 133:209–219.
636 Odion, D. C., M. A. Moritz, and D. A. DellaSala. 2010. Alternative community states maintained by fire in the
637 Klamath Mountains, USA. Journal of Ecology 98:96–105.
638 Olivier, J.-M., M.-J. Dole-Olivier, C. Amoros, G. Carrel, F. Malard, N. Lamouroux, and J.-P. Bravard. 2009. The
639 Rhône River basin. Pages 247–295 Rivers of Europe (Tockner K., Robinson C.T. & Uehlinger U. eds).
640 Elsevier, Amsterdam.
641 Osterkamp, W. R., and C. R. Hupp. 2010. Fluvial processes and vegetation — Glimpses of the past, the present,
642 and perhaps the future. Geomorphology 116:274–285.
643 Oswalt, S. N., and S. L. King. 2005. Channelization and floodplain forests: Impacts of accelerated sedimentation
644 and valley plug formation on floodplain forests of the Middle Fork Forked Deer River, Tennessee, USA.
645 Forest Ecology and Management 215:69–83.
646 Palmer, M. A., E. S. Bernhardt, J. D. Allan, P. S. Lake, G. Alexander, S. Brooks, J. Carr, S. Clayton, C. N. Dahm, J.
647 Follstad Shah, D. L. Galat, S. G. Loss, P. Goodwin, D. D. Hart, B. Hassett, R. Jenkinson, G. M. Kondolf, R.
648 Lave, J. L. Meyer, T. K. O'Donnell, L. Pagano, and E. Sudduth. 2005. Standards for ecologically
649 successful river restoration: Ecological success in river restoration. Journal of Applied Ecology 42:208–
650 217.

651 Perry, L. G., D. C. Andersen, L. V. Reynolds, S. M. Nelson, and P. B. Shafroth. 2012. Vulnerability of riparian
652 ecosystems to elevated CO2 and climate change in arid and semiarid western North America. Global
653 Change Biology 18:821–842.
654 Pickett, S. T. A., S. L. Collins, and J. J. Armesto. 1987. Models, mechanisms and pathways of succession.
655 Botanical Review 53:335–371.
656 Porté, A. J., L. J. Lamarque, C. J. Lortie, R. Michalet, and S. Delzon. 2011. Invasive Acer negundo outperforms
657 native species in non-limiting resource environments due to its higher phenotypic plasticity. BMC
658 Ecology 11:28.
659 Prach, K., and L. R. Walker. 2011. Four opportunities for studies of ecological succession. Trends in Ecology &
660 Evolution 26:119–123.
661 QGIS Development Team. 2015. QGIS Geographic Information System. Open Source Geospatial Foundation
662 Project.
663 R Core Team. 2019. R: A language and environment for statistical computing. R Foundation for Statistical
664 Computing, Vienna, Austria.
665 Räpple, B. 2018. Sedimentation patterns and riparian vegetation characteristics in novel ecosystems on the
666 Rhône River, France: a comparative approach to identify drivers and evaluate ecological potentials.
667 Thèse de Doctorat, Université de Lyon, Lyon.
668 Räpple, B., H. Piégay, J. C. Stella, and D. Mercier. 2017. What drives riparian vegetation encroachment in
669 braided river channels at patch to reach scales? Insights from annual airborne surveys (Drôme River,
670 SE France, 2005-2011). Ecohydrology 10:e1886.
671 Reily, P. W., and W. C. Johnson. 1982. The effects of altered hydrologic regime on tree growth along the
672 Missouri River in North Dakota. Canadian Journal of Botany 60:2410–2423.
673 Schnitzler, A. 1995. Successional status of trees in gallery forest along the river Rhine. Journal of Vegetation
674 Science 6:479–486.
675 Scott, M. L., G. T. Auble, and J. M. Friedman. 1997. Flood dependency of Cottonwood establishment along the
676 Missouri River, Montana, USA. Ecological Applications 7:14.
677 Scott, M. L., P. B. Shafroth, and G. T. Auble. 1999. Responses of riparian Cottonwoods to alluvial water table
678 declines. Environmental Management 23:347–358.

679 Sfair, J. C., V. Arroyo-Rodríguez, B. A. Santos, and M. Tabarelli. 2016. Taxonomic and functional divergence of
680 tree assemblages in a fragmented tropical forest. Ecological Applications 26:1816–1826.
681 Singer, M. B., J. C. Stella, S. Dufour, H. Piégay, R. J. S. Wilson, and L. Johnstone. 2013. Contrasting water-uptake
682 and growth responses to drought in co-occurring riparian tree species. Ecohydrology 6:402–412.
683 Stella, J. C., and J. Bendix. 2018. Multiple stressors in riparian ecosystems. Pages 81–110 Multiple stressors in
684 river ecosystems: status, impacts and prospects for the future (Sabater, S., Elosegi, A., Ludwig, R.,
685 eds.). Elsevier, San Diego.
686 Stella, J. C., L. Kui, G. H. Golet, and F. Poulsen. in review. Modeling riparian forest structure to estimate large
687 wood inputs and other ecosystem services on geomorphically active floodplains. Earth Surface
688 Processes and Landforms.
689 Stella, J. C., J. Riddle, H. Piégay, M. Gagnage, and M.-L. Trémélo. 2013a. Climate and local geomorphic
690 interactions drive patterns of riparian forest decline along a Mediterranean Basin river.
691 Geomorphology 202:101–114.
692 Stella, J. C., P. M. Rodríguez-González, S. Dufour, and J. Bendix. 2013b. Riparian vegetation research in
693 Mediterranean-climate regions: common patterns, ecological processes, and considerations for
694 management. Hydrobiologia 719:291–315.
695 Suding, K. N. 2011. Toward an era of restoration in ecology: successes, failures, and opportunities ahead.
696 Annual Review of Ecology, Evolution, and Systematics 42:465–487.
697 Suding, K. N., K. L. Gross, and G. R. Houseman. 2004. Alternative states and positive feedbacks in restoration
698 ecology. Trends in Ecology & Evolution 19:46–53.
699 Tena, A., H. Piégay, G. Seignemartin, A. Barra, J. F. Berger, B. Mourier, and T. Winiarski. 2020. Cumulative
700 effects of channel correction and regulation on floodplain terrestrialisation patterns and connectivity.
701 Geomorphology 354:107034.
702 Thorel, M., H. Piégay, C. Barthélémy, B. Räpple, C. R. Gruel, P. Marmonier, T. Winiarski, J. P. Bedell, F. Arnaud,
703 G. Roux, J. Stella, G. Seignemartin, A. Tena-Pagan, V. Wawrzyniak, D. Roux-Michollet, B. Oursel, S.
704 Fayolle, C. Bertrand, and E. Franquet. 2018. Socio-environmental implications of process-based
705 restoration strategies in large rivers: should we remove novel ecosystems along the Rhône (France)?
706 Regional Environmental Change 18:2019–2031.

Tonkin, J. D., David. M. Merritt, J. D. Olden, L. V. Reynolds, and D. A. Lytle. 2018. Flow regime alteration degrades ecological networks in riparian ecosystems. Nature Ecology & Evolution 2:86–93.

Van Pelt, R., T. C. O'Keefe, J. J. Latterell, and R. J. Naiman. 2006. Riparian forest stand development along the Queets River in Olympic National Park, Washington. Ecological Monographs 76:277–298.

Vázquez-Tarrío, D., M. Tal, B. Camenen, and H. Piégay. 2019. Effects of continuous embankments and successive run-of-the-river dams on bedload transport capacities along the Rhône River, France. Science of The Total Environment 658:1375–1389.

Walker, L. R., D. A. Wardle, R. D. Bardgett, and B. D. Clarkson. 2010. The use of chronosequences in studies of ecological succession and soil development: Chronosequences, succession and soil development. Journal of Ecology 98:725–736.

Wang, Y., U. Naumann, S. T. Wright, and D. I. Warton. 2012. mvabund - an R package for model-based analysis of multivariate abundance data. Methods in Ecology and Evolution 3:471–474.

Warton, D. I., L. Thibaut, and Y. A. Wang. 2017. The PIT-trap—A "model-free" bootstrap procedure for inference about regression models with discrete, multivariate responses. PloS one 12:e0181790.

Westoby, M. 1998. A leaf-height-seed (LHS) plant ecology strategy scheme. Plant and Soil 199:213–227.

Wilcock, D. N., and C. I. Essery. 1991. Environmental impacts of channelization on the river Main, County Antrim, Northern Ireland. Journal of Environmental Management 32:127–143.

Wright, I. J., P. B. Reich, M. Westoby, D. D. Ackerly, Z. Baruch, F. Bongers, J. Cavender-Bares, T. Chapin, J. H. Cornelissen, M. Diemer, J. Flexas, E. Garnier, P. K. Groom, J. Gulias, K. Hikosaka, B. B. Lamont, T. Lee, W. Lee, C. Lusk, J. J. Midgley, M.-L. Navas, ü. Niinemets, J. Oleskyn, N. Osada, H. Poorter, P. Poot, L. Prior, V. Pyankov, C. Roumet, S. C. Thomas, M. G. Tjoekler, E. J. Veneklaas, and R. Villar. 2004. The worldwide leaf economics spectrum. Nature 428:821–827.

Zanne, A. E., G. Lopez-Gonzales, D. A. Coomes, J. Ilic, S. Jansen, S. L. Lewis, R. B. Miller, N. G. Swenson, M. C. Wiemann, and J. Chave. 2009. Data from: Towards a worldwide wood economics spectrum. Dryad Digital Repository https://doi.org/10.5061/dryad.234.

733 Table 1. Variation in independent and dependent variables between the rivers Drôme (n = 69 plots) and Rhône

734 (n = 65 plots), France (CWM = community-weighted mean, FDis = functional dispersion, SLA = specific leaf

735 area).

Measure	Variable	Drôme River		Rhône River	
		mean (±SD)	range	mean (±SD)	range
Plot description					
	Forest stand age (years)	31.3 (±20.3)	5.0 - 62.0	44.6 (±18.6)	16.0 - 76.0
	Sediment depth (cm)	42 (±36)	0 - 140	249 (±121)	24 - 490
	Mean annual flow (m^3)	18.4 (±4.6)	7.3 - 31.3	527.2 (±402.4)	77.7 - 1550.4
Functional traits					
CWM	SLA	12.63 (±1.66)	10.0 - 17.0	14.87 (±3.00)	11.1 - 21.8
	Wood density	0.41 (±0.05)	0.3 - 0.6	0.47 (±0.10)	0.3 - 0.7
	Seed mass	1.40 (±0.90)	0.4 - 4.2	1.63 (±1.04)	0.2 - 3.8
FDis	SLA	0.24 (±0.20)	0.0 - 0.7	0.40 (±0.26)	0.0 - 1.0
	Wood density	0.51 (±0.39)	0.0 - 1.2	0.69 (±0.44)	0.0 - 1.4
	Seed mass	0.41 (±0.36)	0.0 - 1.4	0.40 (±0.25)	0.0 - 1.1
Stand attributes					
Basal area (m^2 ha^{-1})	Live trees	15.47 (±9.76)	0.1 - 38.7	27.65 (±10.85)	6.3 - 57.8
	Dead trees	3.72 (±3.69)	0.0 - 18.0	5.13 (±4.43)	0.0 - 22.3
	Exotic trees	0.58 (±1.10)	0.0 - 5.2	8.22 (±9.92)	0.0 - 42.8
Mean diameter (cm)	Live trees	17.49 (±4.91)	8.7 - 30.7	24.91 (±8.02)	10.7 - 47.7
	Dead trees	15.60 (±5.63)	9.0 - 44.2	28.96 (±16.97)	9.9 - 76.6
	Exotic trees	13.7 (±4.23)	8.0 - 24.4	17.49 (±6.11)	7.5 - 35.4
Stem density (n ha^{-1})	Live trees	504 (±262.65)	16 - 1066	463 (±241.09)	71 - 1169
	Dead trees	157 (±107.85)	0 - 500	98 (±99.12)	0 - 453
	Exotic trees	38 (±80.39)	0 - 466	276 (±225.97)	0 - 1122
Tree genera					
Basal area (m^2 ha^{-1})	*Populus* spp.	11.44 (±8.87)	0.00 - 38.59	14.83 (±11.90)	0.00 - 43.97
	Fraxinus spp.	1.03 (±1.76)	0.00 - 7.28	1.59 (±2.71)	0.00 - 14.08
	Acer spp.	1.43 (±2.54)	0.00 - 11.74	4.04 (±4.52)	0.00 - 19.10
Mean diameter (cm)	*Populus* spp.	21.22 (±7.27)	8.01 - 43.60	54.15 (±16.20)	26.78 - 113.00
	Fraxinus spp.	13.64 (±3.99)	8.00 - 23.33	23.54 (±12.82)	8.50 - 68.50
	Acer spp.	14.58 (±3.65)	8.00 - 22.00	20.62 (±10.34)	7.50 - 60.50
Stem density (n ha^{-1})	*Populus* spp.	268 (±180.38)	0 - 833	97 (±129.87)	0 - 604
	Fraxinus spp.	53 (±93.35)	0 - 600	58 (±113.75)	0 - 652
	Acer spp.	72 (±128.49)	0 - 633	157 (±162.13)	0 - 636
Diversity indices					
	Diameter classes	1.59 (±0.43)	0.0 - 2.1	1.94 (±0.29)	0.8 - 2.4
	Tree species	0.79 (±0.56)	0.0 - 1.7	0.96 (±0.37)	0.0 - 1.7

736

737 Table 2. Top-ranking models predicting variations in abiotic drivers and biotic responses over time along the
738 rivers Drôme and Rhône, France, as assessed with Akaike's information criterion corrected for small sample
739 size (AIC_c). Other model information provided include the number of estimated parameters including the
740 intercept (k), AIC_c weight (*W*) and adjusted coefficient of determination (R^2). Asterisks in the model formulas
741 indicate an interaction term (CWM = community-weighted mean, FDis = functional dispersion, SLA = specific
742 leaf area).

Measure	Dependent variable	Top-ranked model	k	*W*	R^2
Abiotic drivers					
	Sediment depth	Age * River	5	0.823	0.564
	Mean annual flow	Year * River	5	0.941	0.476
	SD annual flow	Year	5	0.425	0.108
Functional traits					
CWM	SLA	Age * River	5	0.423	0.387
	Wood density	Age * River	5	0.399	0.430
	Seed mass	Age	3	0.282	0.376
FDis	SLA	Age + River	4	0.373	0.232
	Wood density	Age * River	5	0.305	0.228
	Seed mass	Age * River	5	0.500	0.300
Stand attributes					
Basal area	Live trees	Age * River + Sed_depth	6	0.775	0.290
	Dead trees	Age * River + Sed_depth	6	0.978	0.174
	Exotic trees	Age * River + Sed_depth	6	0.962	0.578
Mean diameter	Live trees	Age * River	5	0.632	0.332
	Dead trees	Age*River + Sed_depth	6	0.857	0.155
	Exotic trees	Age*River	5	0.378	0.183
Stem density	Live trees	Age + River + Sed_depth	5	0.612	0.139
	Dead trees	Age * River + Sed_depth	6	0.297	0.117
	Exotic trees	Age + River	4	0.417	0.490
Tree genera					
Basal area	*Populus* spp.	Age * River	5	0.720	0.079
	Fraxinus spp.	Age + Sed_depth	4	0.351	0.228
	Acer spp.	Age * River + Sed_depth	6	0.584	0.344
Mean diameter	*Populus spp.*	Age*River	5	0.482	0.706
	Fraxinus spp.	Age + River	4	0.407	0.295
	Acer spp.	Age + River + Sed_depth	5	0.574	0.182
Stem density	*Populus* spp.	Age * River	5	0.617	0.328
	Fraxinus spp.	Age + Sed_depth	4	0.457	0.180
	Acer spp.	Age * River + Sed_depth	6	0.944	0.397
Diversity indices					
	Diameter classes	Age * River	5	0.435	0.241
	Tree species	Age * River	5	0.731	0.247

743

744 Table 3. Standardized coefficient estimates (±SE) and confidence intervals (95% CI) for each variable used to predict mean and dispersion of functional trait values, basal
745 area, mean diameter and stem density of stand attributes and of tree genera as well as diversity indices to forest stand age along the rivers Drôme and Rhône, France. Bold
746 font indicates coefficient estimates for which the 95% confidence interval excludes zero (CWM = community-weighted mean, FDis = functional dispersion, SLA = specific leaf
747 area).

Measure	Variable	Age		River		Age*River		Sed_depth	
		Estimate (±SE)	(95% CI)	Estimate (±SE)	(95% CI)	Estimate (±SE)	(95% CI)	Estimate (±SE)	(95% CI)
Functional traits									
CWM:	SLA	**0.052 (±0.017)**	**(0.019; 0.085)**	**0.095 (±0.026)**	**(0.044; 0.146)**	**0.069 (±0.026)**	**(0.018; 0.120)**	NA	NA
	Wood density	**0.075 (±0.017)**	**(0.042; 0.108)**	**0.065 (±0.025)**	**(0.016; 0.114)**	**0.060 (±0.025)**	**(0.011; 0.109)**	NA	NA
	Seed mass	**0.603 (±0.067)**	**(0.472; 0.734)**	NA	NA	NA	NA	NA	NA
FDis:	SLA	**0.073 (±0.014)**	**(0.046; 0.100)**	**0.062 (±0.029)**	**(0.005; 0.119)**	NA	NA	NA	NA
	Wood density	**0.162 (±0.029)**	**(0.105; 0.219)**	0.039 (±0.044)	(-0.047; 0.125)	**-0.092 (±0.044)**	**(-0.178; -0.006)**	NA	NA
	Seed mass	**0.167 (±0.022)**	**(0.124; 0.210)**	-0.065 (±0.034)	(-0.132; 0.002)	**-0.113 (±0.034)**	**(-0.180; -0.046)**	NA	NA
Stand attributes									
Basal area:	Live trees	**0.365 (±0.100)**	**(0.169; 0.561)**	0.413 (±0.218)	(-0.014; 0.840)	**-0.567 (±0.153)**	**(-0.867; -0.267)**	**0.256 (±0.119)**	**(0.023; 0.489)**
	Dead trees	**0.270 (±0.087)**	**(0.099; 0.441)**	-0.343 (±0.188)	(-0.711; 0.025)	**-0.452 (±0.132)**	**(-0.711; -0.193)**	**0.379 (±0.103)**	**(0.177; 0.581)**
	Exotic trees	-0.003 (±0.086)	(-0.172; 0.166)	**0.798 (±0.186)**	**(0.433; 1.163)**	**0.461 (±0.130)**	**(0.206; 0.716)**	**0.304 (±0.101)**	**(0.106; 0.502)**
Mean tree diameter:	Live trees	0.064 (±0.034)	(-0.003; 0.131)	**0.373 (±0.051)**	**(0.273; 0.473)**	**-0.209 (±0.051)**	**(-0.309; -0.109)**	NA	NA
	Dead trees	0.077 (±0.051)	(-0.023; 0.177)	**0.374 (±0.107)**	**(0.164; 0.584)**	**-0.356 (±0.077)**	**(-0.507; -0.205)**	**0.141 (±0.058)**	**(0.027; 0.255)**
	Exotic trees	0.033 (±0.053)	(-0.071; 0.137)	**0.159 (±0.069)**	**(0.024; 0.294)**	0.123 (±0.070)	(-0.014; 0.260)	NA	NA
Stem density:	Live trees	**0.147 (±0.061)**	**(0.027; 0.267)**	**-0.560 (±0.165)**	**(-0.883; -0.237)**	NA	NA	**0.280 (±0.089)**	**(0.106; 0.454)**
	Dead trees	**0.513 (±0.181)**	**(0.158; 0.868)**	**-1.449 (±0.394)**	**(-2.221; -0.677)**	-0.409 (±0.276)	(-0.950; 0.132)	0.391 (±0.215)	(-0.030; 0.812)
	Exotic trees	-0.024 (±0.154)	(-0.326; 0.278)	**3.327 (±0.307)**	**(2.725; 3.929)**	NA	NA	NA	NA
Tree genera									
Basal area:	*Populus* spp.	0.143 (±0.115)	(-0.082; 0.368)	0.248 (±0.172)	(-0.089; 0.585)	**-0.594 (±0.173)**	**(-0.933; -0.255)**	NA	NA
	Fraxinus spp.	**0.372 (±0.060)**	**(0.254; 0.490)**	NA	NA	NA	NA	-0.095 (±0.060)	(-0.213; 0.023)
	Acer spp.	**0.476 (±0.089)**	**(0.302; 0.650)**	0.181 (±0.192)	(-0.195; 0.557)	**-0.347 (±0.135)**	**(-0.612; -0.082)**	**0.212 (±0.105)**	**(0.006; 0.418)**
Mean tree	*Populus* spp.	**0.142 (±0.039)**	**(0.066; 0.218)**	**0.909 (±0.058)**	**(0.795; 1.023)**	**-0.124 (±0.059)**	**(-0.240; -0.008)**	NA	NA

diameter:	*Fraxinus* spp.	**0.131 (±0.048)**	**(0.037; 0.225)**	**0.392 (±0.092)**	**(0.212; 0.572)**	NA	NA	NA	NA
	Acer spp.	**0.177 (±0.051)**	**(0.077; 0.277)**	**0.448 (±0.127)**	**(0.199; 0.697)**	NA	NA	**-0.135 (±0.063)**	**(-0.258; -0.012)**
Stem density:	*Populus* spp.	-0.004 (±0.151)	(-0.300; 0.292)	**-1.380 (±0.226)**	**(-1.823; -0.937)**	**-0.606 (±0.228)**	**(-1.053; -0.159)**	NA	NA
	Fraxinus spp.	**1.062 (±0.191)**	**(0.688; 1.436)**	NA	NA	NA	NA	**-0.605 (±0.191)**	**(-0.979; -0.231)**
	Acer spp.	**1.506 (±0.228)**	**(1.059; 1.953)**	0.159 (±0.496)	(-0.813; 1.131)	**-1.483 (±0.347)**	**(-2.163; -0.803)**	**0.755 (±0.270)**	**(0.226; 1.284)**
Diversity indexes									
	Diameter classes	**0.159 (±0.043)**	**(0.075; 0.243)**	**0.284 (±0.065)**	**(0.157; 0.411)**	**-0.133 (±0.065)**	**(-0.260; -0.006)**	NA	NA
	Tree species	**0.330 (±0.052)**	**(0.228; 0.432)**	0.048 (±0.077)	(-0.103; 0.199)	**-0.277 (±0.078)**	**(-0.430; -0.124)**	NA	NA

748 Figure 1. Map of the study area within the Rhône River basin (A); location of the study reaches along the Drôme
749 and Rhône rivers (B); and examples of aerial photograph series showing the riparian forest development along
750 the two rivers (C, aerial photographs: IGN).

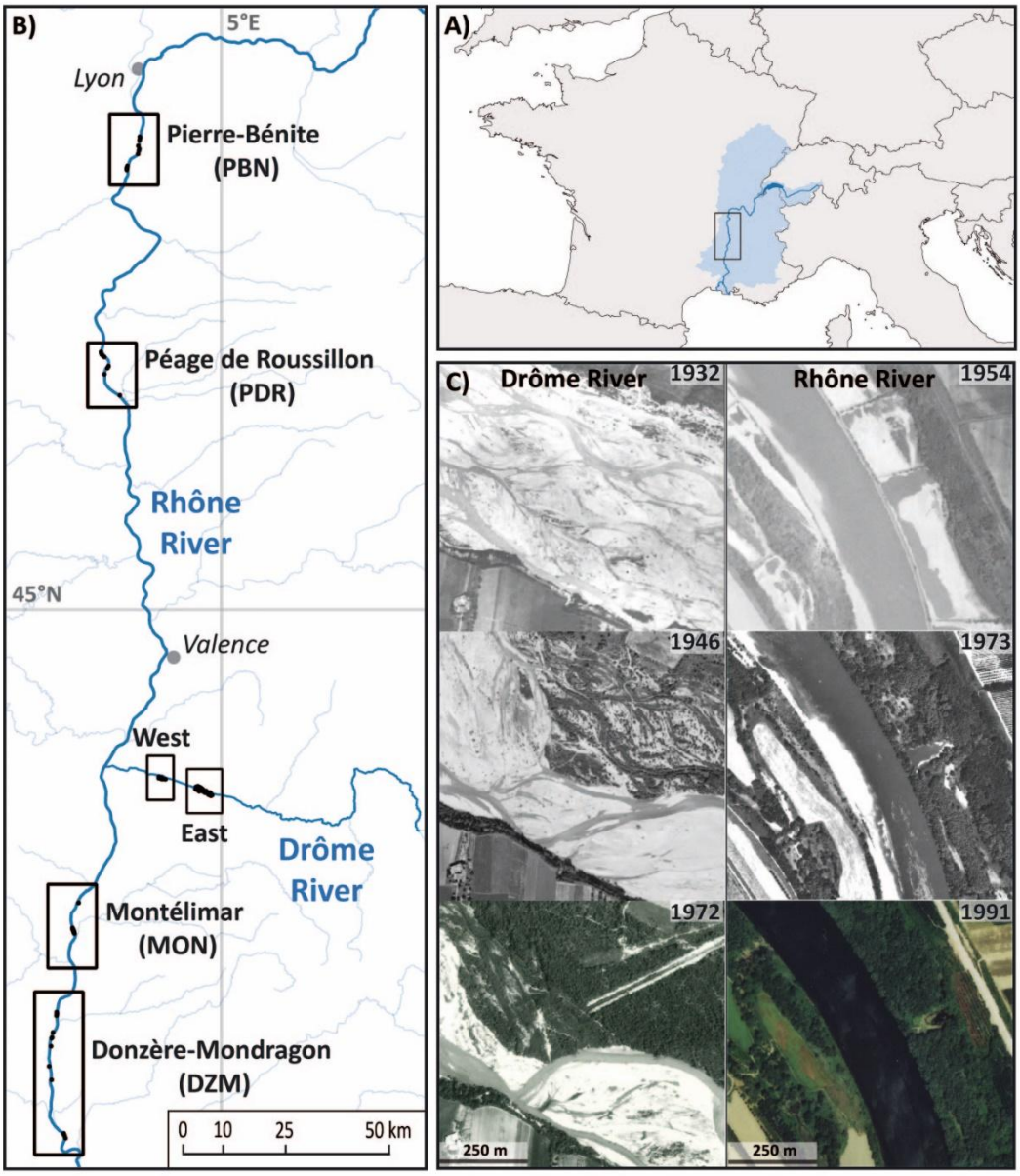

Figure 2. Variation in fine sediment depth with forest stand age along the rivers Drôme and Rhône and trends in the mean and standard deviation (SD) of annual flow since 1940. Annual flow variables were standardized to account for differences in basin size between rivers (n.s. interaction = non-significant Year x River interaction; see Appendix S8). To facilitate interpretation, the dates of commissioning of the diversion canals are shown with arrows in the figure (i.e., DZM = 1952, MON = 1957, PBN = 1966, PDR = 1977).

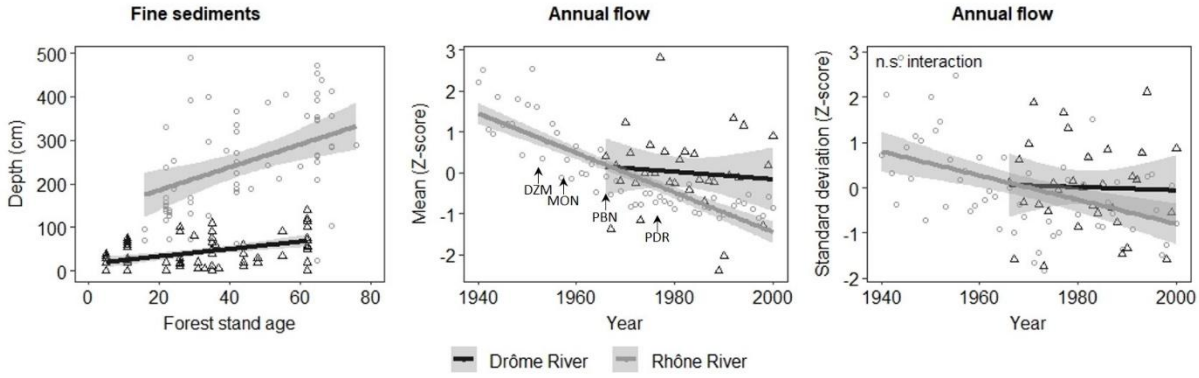

Figure 3. Variation in the mean (CWM) and dispersion (FDis) of specific leaf area (SLA, m^2 kg^{-1}), wood density (g cm^3) and seed mass (mg) with forest stand age along the rivers Drôme and Rhône (n.s. interaction = non-significant Age x River interaction; see Table 3). Trait values and their variation increased more rapidly along the Rhône River for SLA and wood density, compared to the Drôme.

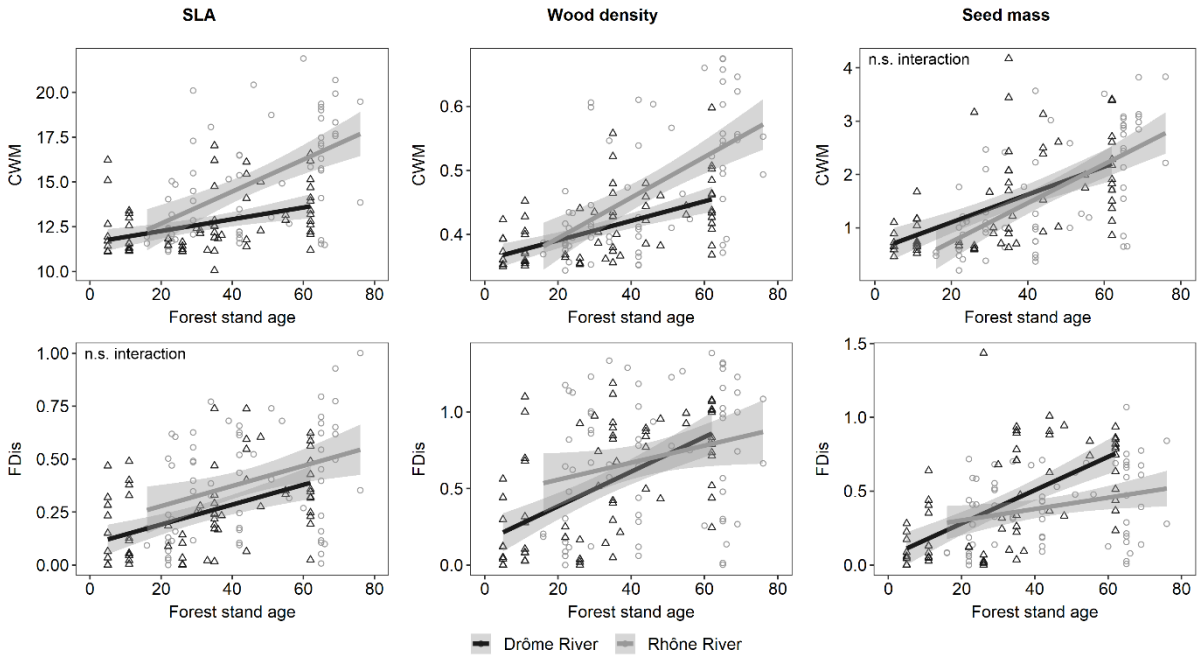

760 Figure 4. Variation in the basal area, mean diameter and stem density of live, dead and exotic tree species with

761 forest stand age along the rivers Drôme and Rhône (n.s. interaction = non-significant Age x River interaction;

762 see Table 3). Basal area increased much more rapidly within the Rhône riparian forest for live trees and for the

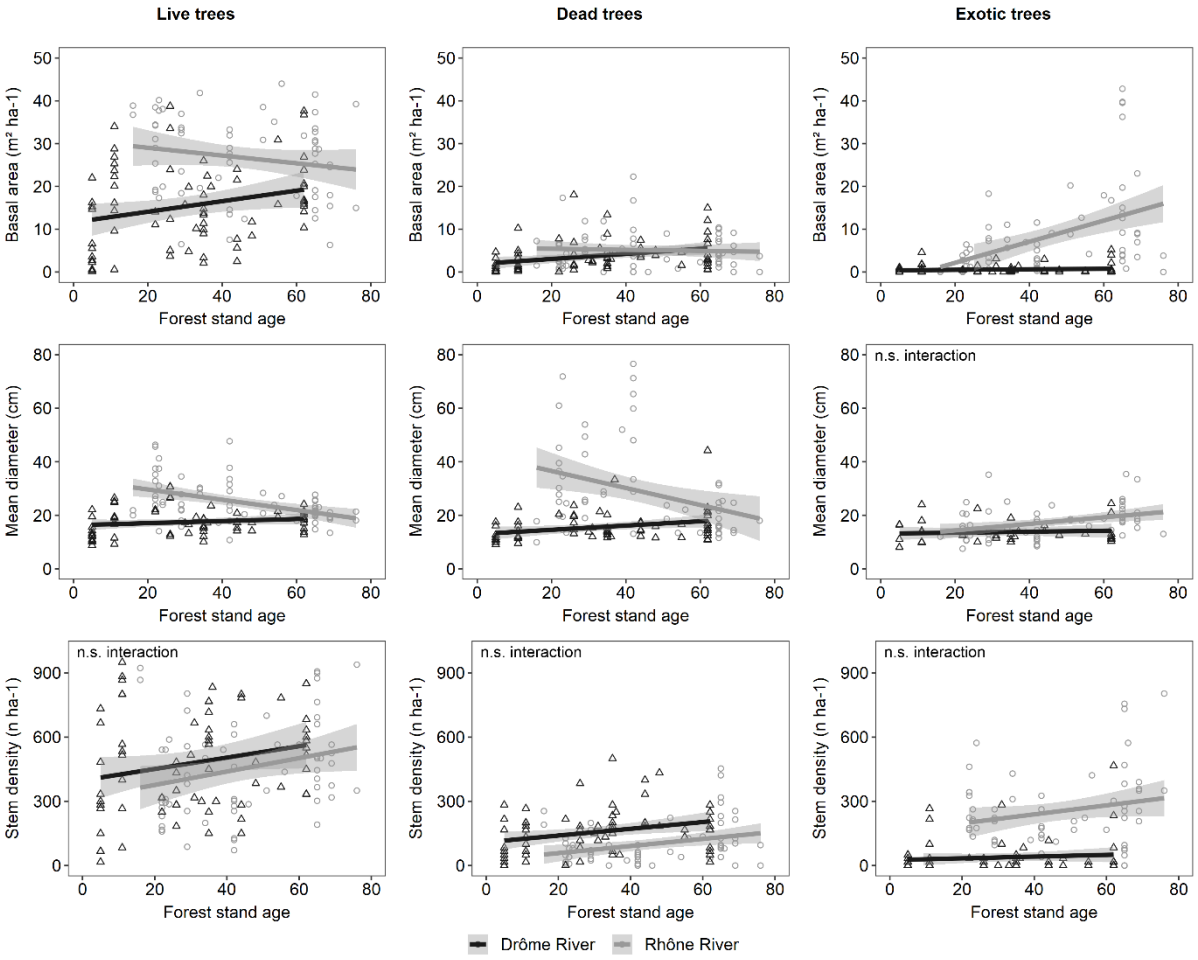

763 exotic species fraction, largely due to more large trees in early to mid-successional phases.

764 Figure 5. Variation in the basal area, mean diameter and stem density of *Populus* spp.*, Fraxinus,* spp. and *Acer*
765 spp. with forest stand age along the rivers Drôme and Rhône (n.s river = non-significant River effect; see Table
766 3). Whereas development of *Fraxinus* spp., a native post-pioneer taxon, was comparable among rivers, the
767 overall divergence in successional trajectories (Figure 4) was driven by greater *Populus* spp. tree size and basal
768 area, as well as the higher density and basal area of non-native *Acer* species, primarily *Acer negundo*, within the

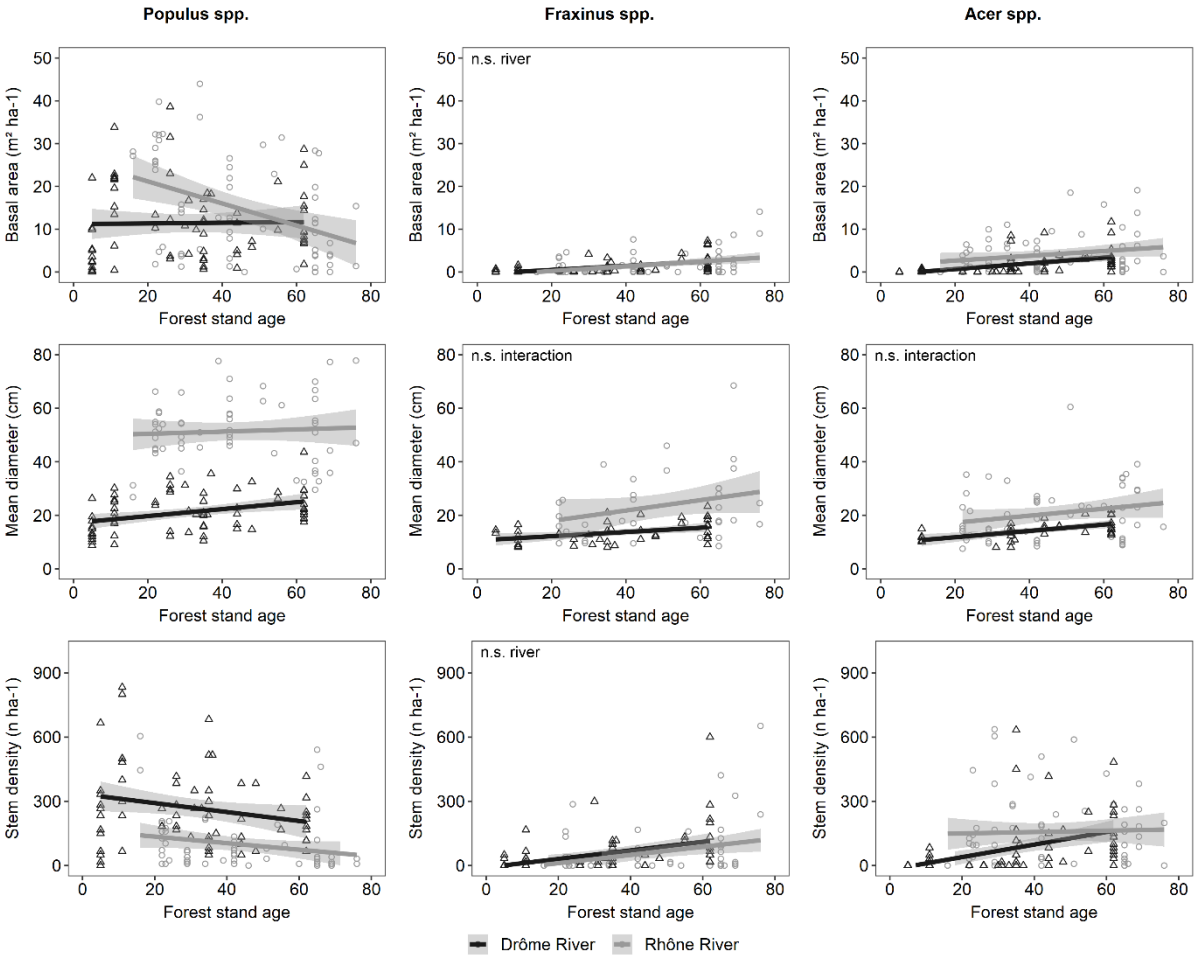

769 Rhône River riparian forest community.

770 Figure 6. Variation in the diversity of tree diameter classes and tree species with forest stand age along the

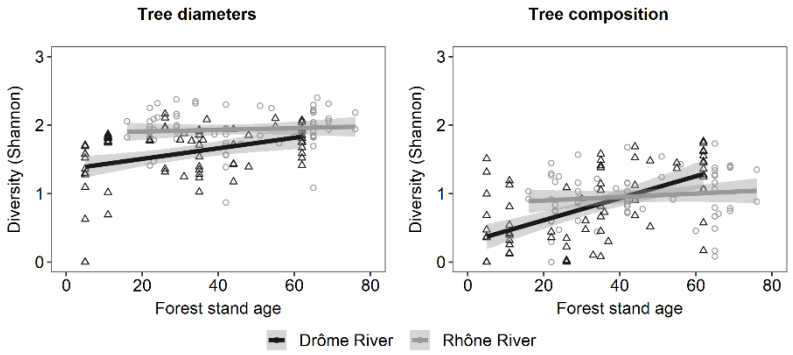

771 rivers Drôme and Rhône.

Figure 7. Constrained canonical analysis of principal coordinates of A) tree diameter classes and B) tree species in riparian forests along the rivers Drôme and Rhône. To facilitate graphical interpretation, data are grouped into three classes of forest stand age (<25, 25-50 and >50 years). In addition, the centroids in principle coordinate space of the three most influential diameter classes ("70" is DBH > 70 cm; "52.5" is 51 cm < DBH < 56 cm; "12.5" is 11 cm < DBH < 16 cm) and tree species (Acer.neg is *Acer negundo*, Sal.alb is *Salix alba*, Sam.nig is *Sambucus nigra*) are provided (see Appendix S9 and S10).

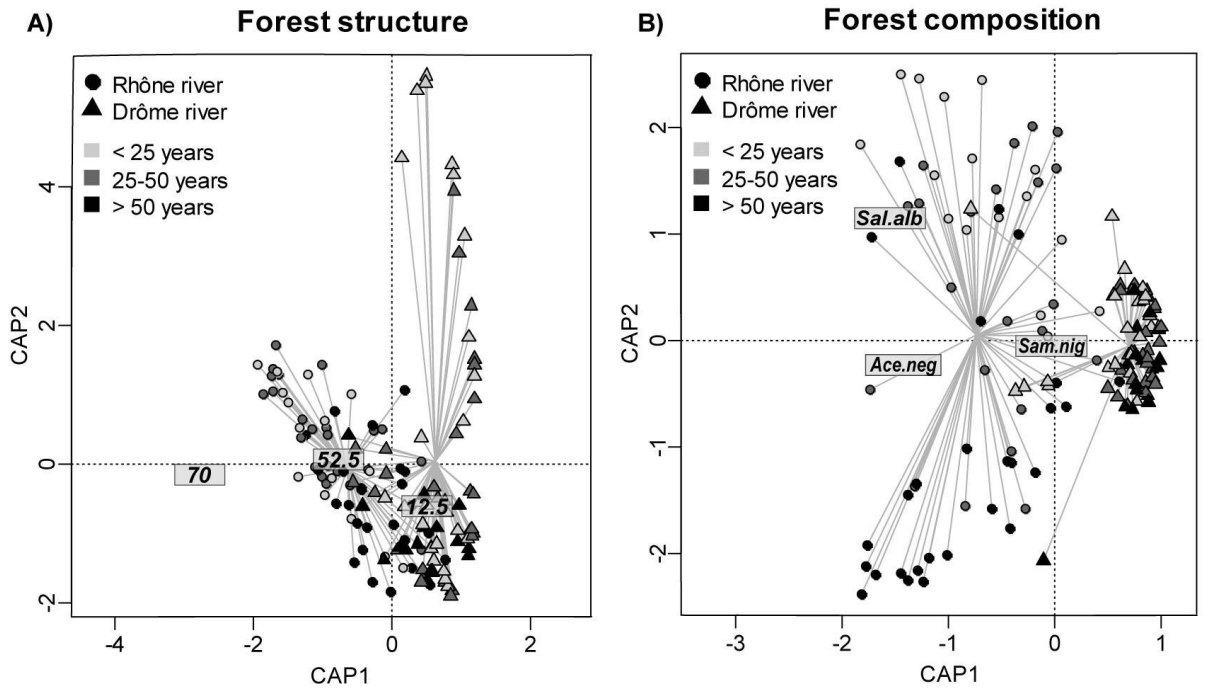

778 Figure 8. Conceptual model of ecological trajectory of riparian forests between the channelized and regulated

779 Rhône River and the relatively unmodified Drôme River, across a range of successional phases in eastern

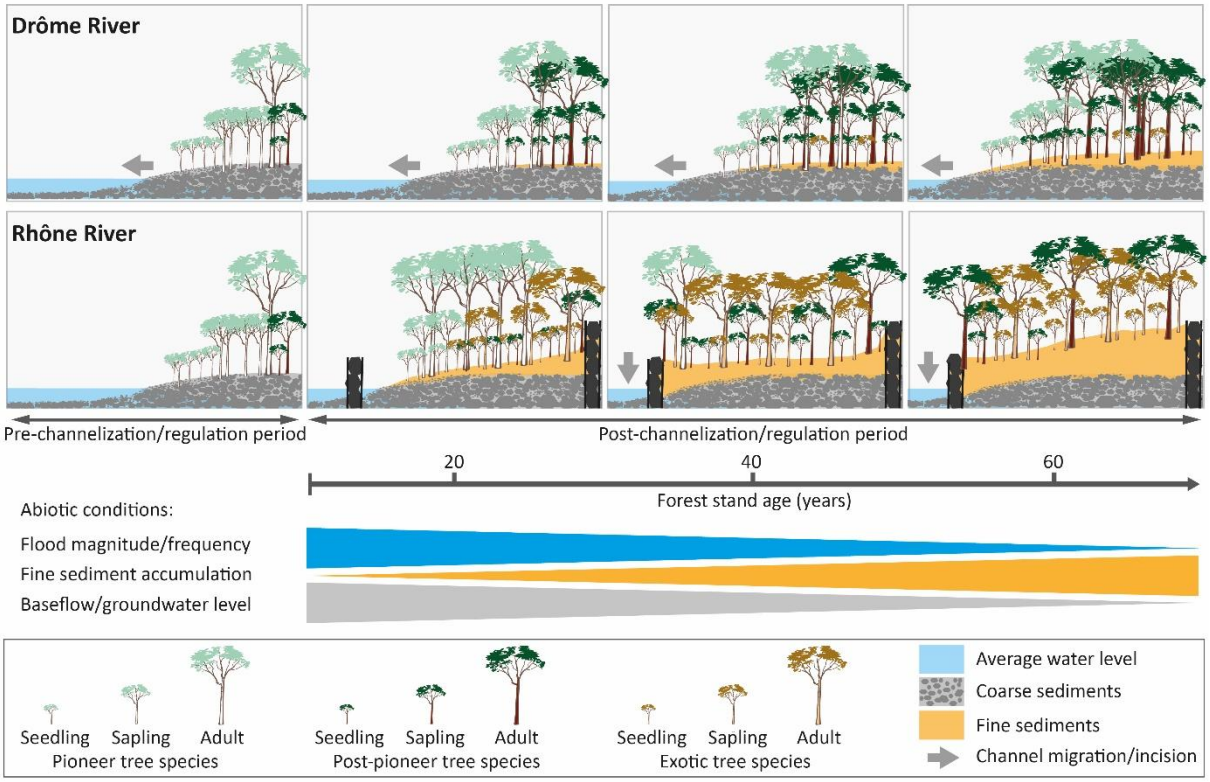

780 France.